

High-resolution electrophysiology on a chip: Transient dynamics of alamethicin channel formation

Markus Sondermann^a, Michael George^b, Niels Fertig^b, Jan C. Behrends^{a,*}

^a Department of Physiology, Albert-Ludwigs-Universität Freiburg, Hermann-Herder-Str. 7, 79104 Freiburg, Germany

^b Nanion Technologies GmbH, Pettenkoferstr. 12, 80336 München, Germany

Received 18 January 2006; received in revised form 16 March 2006; accepted 16 March 2006

Available online 17 April 2006

Abstract

Microstructured planar substrates have been shown to be suitable for patch clamp recording from both whole cells and isolated patches of membrane, as well as for measurements from planar lipid bilayers. Here, we further explore this technology with respect to high-resolution, low noise single-channel recording. Using solvent-free lipid bilayers from giant unilamellar vesicles obtained by electro-swelling, we recorded channels formed by the peptaibol alamethicin, a well-studied model system for voltage-dependent channels, focusing on the transient dynamics of single-channel formation upon application of a voltage step. With our setup, we were able to distinctly resolve dwell times well below 100 μ s and to perform a thorough statistical analysis of alamethicin gating. Our results show good agreement with models that do not rely on the existence of non-conducting preaggregate states. Microstructured apertures in glass substrates appear promising with respect to future experiments on cellular ion channels reconstituted in suspended lipid membranes.

© 2006 Elsevier B.V. All rights reserved.

Keywords: Patch clamp chip; Glass microstructure; Lipid bilayer; Electrophysiology; Alamethicin

1. Introduction

Patch clamping with pipettes has been the standard technique for measuring current signals from ion channels of cell membranes over the last three decades [1]. Recently, several reports on ion channel recordings using planar substrates, or ‘patch clamp chips’, have been published. These include recordings from whole cells [2,3], single channels in cell-attached mode [3,4], single channels in painted bilayers [2,5,6], bilayers obtained from lipid monolayers [6], and in bilayers produced from giant unilamellar vesicles (GUVs) prepared from charged lipids [7]. A recent review of such experiments [8] also stresses the potential of the ‘patch clamp on chip’-technology for single channel recordings with enhanced resolution.

Both amplitude- and time-resolution (usable bandwidth) in a voltage clamp experiment are strongly dependent on the total capacitance of the recording situation [9,6,3]. As far as

bandwidth is concerned, low access resistances can compensate the high capacitance (>100 pF) of conventional bilayers, enabling in a few instances resolution of sub-millisecond large-amplitude single channel events [10] or application of step changes in bilayer voltage [11–13]. However, large total capacitance introduces dominant noise at higher frequencies even with very low access resistances, because current noise is either independent of access resistance or, in the case of $R_e C_p$ -noise (in the terminology of Ref. [9]) scales with its square root. Minimizing the total capacitance (contributed by membrane, pipette, electrode, holder and amplifier) is thus most efficient in reducing noise as well as in increasing the usable bandwidth of the recording. For instance, micro-bilayers on 2–5 μ m diameter pipette tips have been used to obtain excellent noise performance in recording gramicidin channels [14]. In addition to small aperture size and, therefore, low bilayer capacitance, the microstructured planar glass substrates we have developed appear to offer particular advantages: solution volumes needed to make contact with the electrodes are in the range of a few microliters. Hence, the surface of the chip that is covered by solution is small. Also, the thickness of the glass material

* Corresponding author. Fax: +49 761 203 5147.

E-mail address: jan.behrends@physiologie.uni-freiburg.de (J.C. Behrends).

surrounding the aperture is at least 50 μm . In these ways, the capacitance of the substrate holding the bilayer as well as that of the bilayer itself is kept small.

We have previously shown that it is possible to obtain suspended planar bilayers on patch clamp apertures in glass chips by painting of lipid-solutions in decane and to record channels formed by gramicidin [15] and alamethicin [2] with good resolution. However, we noted that with the smallest apertures that should afford the best noise performance, it became more difficult to reliably obtain bilayers by the painting method. To be able to further explore high-resolution bilayer recording on our device, we therefore adopted the alternative approach of forming solvent-free suspended bilayers from giant unilamellar vesicles. The method is similar to that pioneered in Ref. [7] to form bilayers on an aperture in a $\text{SiO}_2/\text{Si}_3\text{N}_4$ diaphragm, except that we obtained GUVs by electroformation [16] and that we positioned them on the aperture by suction rather than electrophoresis. This allowed us to make use of the apparatus and software developed for automated patch clamp recording from cells [17], and essentially obtain suspended planar bilayers in an automated fashion.

In order to test our current system, we have performed a series of experiments on alamethicin channels in phospholipid membranes. Alamethicin is a well-studied peptide (see, e.g., Refs. [18–20] for review) that has served as a paradigm of a voltage gated channel since decades. Typical features of alamethicin are voltage-dependent conductance, the existence of multiple non-equidistant conductance levels of a single channel and its macroscopic dipole moment (e.g., [18,19] and references cited therein). There is a plethora of reports on alamethicin single-channel steady-state characteristics including studies on transient current dynamics after stepwise changes of the membrane potential, some of them treating macroscopic conductance properties [21–26] and some being concerned with single channels [11–13]. In Ref. [11], alamethicin was incorporated into a lecithin bilayer, obtained from lipid dissolved in octane, and a small membrane patch of 10 μm diameter was isolated by touching a glass pipette against the bilayer. The authors of Ref. [13] have produced a small bilayer patch at the tip of a patch clamp pipette by passing it through a lipid monolayer.

These rather intricate methods of forming small bilayers are unnecessary in experiments with glass chips as they are used here. By combined use of the techniques outlined above, we were able to demonstrate the feasibility of low noise recordings of single-channel formation in lipid bilayers with high temporal resolution in a relatively simple setup using readily available components. Modifications of this setup seem promising for further extension of the resolution boundaries of bilayer electrophysiology.

2. Materials and methods

2.1. Electrophysiology

All experiments were performed with the Port-a-Patch automated patch clamp system from Nanion Technologies (Munich, Germany) using *NPC-1* borosilicate glass chips with an aperture of approximately 1 μm . The resistance of the apertures was approximately 1 M Ω in 500 mM KCl

solution and the chip capacitance was roughly approximated to be on the order of 0.5 pF. The total capacitance of the setup without the chip was 4.4 pF, of which 1.3 pF were due to the amplifier input and 3.1 pF to the other components of the Port-a-Patch system. Current signals were recorded and amplified by an EPC-8 amplifier from HEKA Elektronik (Lambrecht, Germany). The system was computer controlled by the *PatchControl*TM software (Nanion) and GePulse (Michael Pusch, Genoa, Italy, http://www.ge.cnr.it/ICB/conti_moran_pusch/programs-pusch/software-mik.htm).

The data were filtered using the built-in Bessel filter of the EPC-8 at a cut-off frequency of 30 kHz and digitized at a sampling rate of 200 kHz using a PCI-6036E card (16 bit resolution, -10 V to $+10$ V voltage range) from National Instruments (Austin, TX). Symmetrical salt solutions of 500 mM KCl, 2 mM HEPES, pH 7.4 were used for all experiments, unless mentioned otherwise. 1 μM alamethicin (Sigma, Steinheim, Germany, product no. A4665) in the same salt solution was added to the upper compartment of the chip after a seal had been formed. The alamethicin solution contained the Rf30 as well as the Rf50 analogue. All applied voltages given in the text are voltages applied to the lower compartment of the chip (see Fig. 1A). The experiments were performed at room temperature. The acquired data were analyzed by custom-made software written in PV-Wave (Visual Numerics, Inc., San Ramon, CA).

2.2. Bilayer formation

The lipid bilayers were obtained from giant unilamellar vesicles (GUVs), which were positioned onto the chip aperture by application of negative pressure. The GUVs burst as soon as they touch the glass surface of the chip and form a bilayer that spans the aperture. An example of the seal formation process

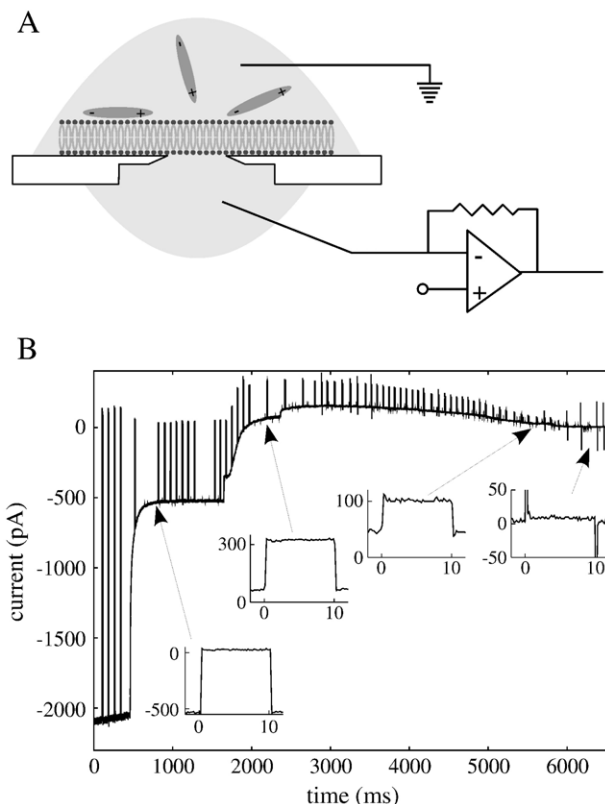


Fig. 1. (A) Schematic drawing of the experimental setup. After formation of a seal, alamethicin (ellipsoids) is added to the upper compartment. (B) Example of the seal formation process. A voltage of -10 mV and negative pressure is supplied to the lower compartment of the chip. In this case, both compartments are filled with 85 mM KCl solution and a suspension of vesicles filled with 200 mM D-Sorbitol is added to the upper compartment. The negative pressure is continuously increased until a predetermined seal resistance is achieved and then set to 0. The insets show the responses to a test pulse of 10 mV amplitude.

is illustrated in Fig. 1B. The GUVs were prepared by electrosweeling [16]. 10 μl of 0.25 mM lipid solution (see below) were deposited onto an indium tin oxide (ITO) coated glass plate and evaporated for 1 h at 15 kPa. A nitrile ring was placed around the dried lipid film and filled with 230 μl of 1 M D-Sorbitol dissolved in deionized water. A second ITO coated glass plate was placed on top of the ring. An AC voltage of 4 V peak-to-peak amplitude and a frequency of 5 Hz was supplied to the ITO slides over a period of 4 h at room temperature. After successful swelling the vesicles were stored in a plastic vessel at a temperature of 4 $^{\circ}\text{C}$ until use or used immediately. In all experiments 1,2-Diphytanoyl-*sn*-Glycero-3-Phosphocholine (DPhPC) from Avanti Polar Lipids (Alabaster, AL) was used. The lipid was dissolved in a mixture of methanol (10%) and diethyl ether (90%). In some of the experiments, the lipid solution contained 10 mol% of cholesterol (SIGMA, Steinheim, Germany) and/or 250 nM 1,2-dimyristoyl-*sn*-glycero-3-phosphoethanolamine-tetramethylrhodamine. Based on the aperture diameter of the chips and a specific capacitance of DPhPC of $0.5 \mu\text{F}/\text{cm}^2$ [27] the membrane capacitance can be estimated to be on the order of 4 fF.

3. Results

Since our aim was to perform recordings with high temporal resolution, a filter frequency of 30 kHz and an amplifier gain of 20 mV/pA were chosen as a compromise between noise, temporal resolution and measurable current range. At this gain (500 M Ω feedback resistor), the unconnected amplifier headstage produced a noise current of 4.3 pA root mean-square (rms) when the amplifier lowpass Bessel filter was set to 30 kHz. This value was reduced to 1 pA with higher gain settings (50 G Ω feedback resistor), where, however, the amplifier would have been saturated by currents greater than 200 pA. When the headstage was connected to the Port-a-Patch measuring station (without the glass chip), the noise was 4.9 pA rms at 20 mV/pA, and 2.7 pA rms at 50 mV/pA (30 kHz).

Fig. 2A displays the current response of a DPhPC bilayer with alamethicin to the application of one voltage pulse from 0 mV to -100 mV. The seal resistance was 14 G Ω . The total noise current was 5 pA (rms) for the chosen settings of the amplifier low pass Bessel filter (30 kHz) and the amplifier gain (20 mV/pA). By selecting an amplifier gain of 50 mV/pA, the noise could be reduced to 2.7 pA and further to 1 pA rms by setting the Bessel filter to 10 kHz (not shown).

The beginning of the voltage pulse is shown in detail in Fig. 2B. In order to ensure a correct detection of possible channel openings at the very beginning of the pulses, the remaining capacitive transients were subtracted numerically during data analysis. For this purpose, pulses with the same amplitude but opposite polarity were applied to the bilayer in such a way that no channels were active. The average of these pulses was added to the current traces of interest. In order to preserve absolute current values, the current corresponding to the leak conductance was re-added afterwards. The final result of this operation is shown as the gray trace in Fig. 2B.

Fig. 2C displays a magnification of one single-channel opening. The typical pattern of different non-equidistant conductance states of a single alamethicin channel is clearly resolved (see also the histogram in Fig. 2D and discussion below).

Obviously, sojourns in a certain conductance state with dwell times well below 100 μs can be captured by the setup. Assuming that the temporal resolution is limited by the low pass filter

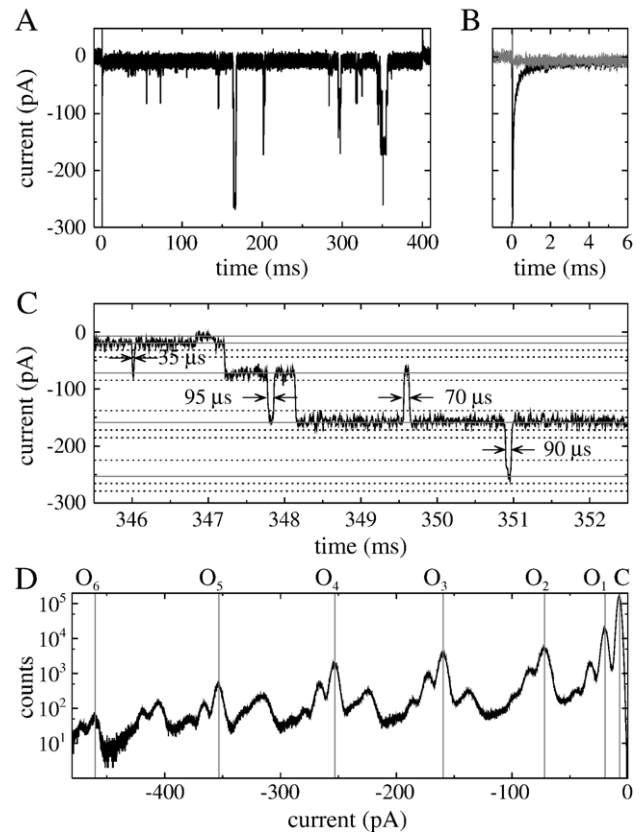


Fig. 2. Current signal recorded from a DPhPC bilayer. At 0 ms, the voltage is increased from 0 to -100 mV for 400 ms. The total alamethicin concentration in solution is 500 nM. (A) Complete pulse. (B) Beginning of the pulse (black trace). The gray trace is obtained by numerically compensating the capacitive transient (see text for details). (C) Magnification of a part of (A). The gray lines denote the different single-channel conductance levels. The dotted lines denote current values that correspond to cases where more than one channel is open. (D) All-points current histogram including the data of 220 runs of the experiment. The non-conducting state is denoted by a 'C', the conducting single-channel states are denoted by 'O_{1–6}'.

setting of 30 kHz, the corresponding 10–90% rise time [28] of 11 μs and the sampling rate of 200 kHz would allow one to recognize sojourns of 25 μs duration. With a sampling interval of 5 μs , we were not able to correctly resolve 10–90% rise times of single channel transitions, as there were never more than 3 data points during a transition. The upper limit of observed transition times is thus 15 μs , i.e., less than one sampling interval larger than the theoretical minimum rise time set by the filter. On the basis of these measurements, we would not feel confident in making the decision as to whether the rise times were limited by the filter or by the RC characteristics of our setup. Using the relation $B_{\text{max}} = (2\pi RC)^{-1}$ [9], with a total capacitance of $C = 4.9$ pF (see Materials and methods) and an access resistance of $R = 1$ M Ω , the maximum bandwidth B_{max} of our recordings would be estimated to be only slightly above 30 kHz.

The conductance of alamethicin single-channel levels depended approximately quadratically on the order of the respective level. This is in qualitative agreement with theoretical estimations [29,30]. However, as is obvious from the current histogram prepared from a total of 88 s (220 sweeps) of data

(Fig. 2D), there are also further conductance levels that do not fit this parabolic dependence. These conductance levels suggest the simultaneous opening of more than one single channel. This hypothesis is supported by the fact that all of the current values corresponding to these levels closely match linear combinations of the ‘true’ single channel levels that are denoted by gray lines in Fig. 2C, D. As can be inferred from the histogram, there are incidents when at least three channels are open simultaneously.

Further statistical analysis is presented in Fig. 3. Panel (A) displays the response of the alamethicin channels to a -100 mV voltage pulse averaged over 220 trials. The average response has a sigmoidal shape. The current does not increase directly after application of the voltage step. Instead, there is a delay (approximately 6 ms in the case of Fig. 3), before the current increases. This is in good correspondence with macroscopic, i.e., multi-channel measurements of alamethicin currents in lipid bilayers as reported in, e.g., [22,23].

Fig. 3B shows the probability distribution of the delay between the application of the voltage step and the first channel opening. The distribution has a pronounced maximum at about 7 ms. This is in good agreement with the turn-on-delay obtained from the average current response. The probability distribution of the conductance state which is entered first is displayed in Fig. 3C. With a probability of 0.982, i.e., almost always, it is the lowest conductance state (O_1) that is entered first. This value was reproduced in other experiments (0.96 ± 0.05 , $n=9$), regardless of the fact that voltage, lipid composition or alamethicin concentration were changed in these experiments. With a probability of a few percent, the conductance state entered first is the second lowest conductance state (O_2). There are some rare events where the first current flow occurs through a conductance state that corresponds to more than one open channel.

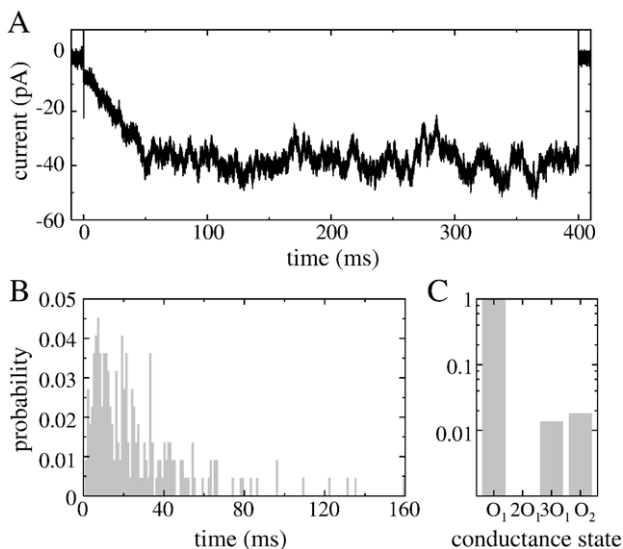


Fig. 3. (A) Average trace obtained from 220 runs as in Fig. 2A. (B) Probability distribution of the time spans from the application of the voltage step until the first channel opening. (C) Probability distribution of the conductance level that is entered as the first one after the application of the voltage step. The terms ‘ O_N ’ denote the N th conductance level as defined in Fig. 2. The term ‘ nO_N ’ denotes a conductance of n times the one of ‘ O_N ’. Note that the probability of the first opening being in $3O_1$ or O_2 corresponds to 3 or 4 events, respectively.

It has been stated in the literature that the transitions between the different alamethicin conductance states always occur between adjacent states [19,31]. Thanks to the high temporal resolution of the planar chip setup, we were able to perform a detailed statistical test of this statement. For the sake of simplicity and clarity, only the ‘true’ single-channel conductance levels, i.e., those labeled in Fig. 2D were taken into account: First, the conductance state was determined for every measured point. We then checked whether it corresponded to a single-channel conductance level or to a cumulated conductance of multiple open channels. In the latter case, the detected state was projected onto a single-channel state. For example, if the system was detected to be in a state corresponding to the linear sum of O_3 (one channel) and O_1 (a second channel), then the second channel was disregarded, i.e., the system was considered to consist of a single channel in the state O_3 . This procedure is firstly justified by the fact that the probability of finding the system in a state that corresponded to only one open channel was 74% (relative to all open states), so that possible errors would be small. More importantly, however, in transitions between states such as from $O_3 + O_1$ to $O_4 + O_1$ the state O_1 of the second channel does not change and can be neglected.

Exemplary results of such an analysis for the data presented in Fig. 2 are shown in Fig. 4. The majority of the transitions into a certain state is from adjacent conductance levels. For example, the probability that state O_3 is entered either from state O_2 or state O_4 is 0.97. With exception of state O_6 , the probability $P_{\text{adj},s}$ ($s=C, O_1, \dots$) for a state to be entered from an adjacent state is approximately of the same magnitude. For state O_6 , this probability is approximately 0.82. On average, the probability that a conductance state is entered from an adjacent state is $\langle P_{\text{adj},s} \rangle_s = 0.95 \pm 0.06$.

Obviously, there is also a finite probability for transitions from second-next states to a single state under consideration. An example is depicted in Fig. 4H. Furthermore, there are also transitions where more than one state is omitted. However, such transitions occur very scarcely. Performing the statistics over all transitions and states, the probability of observing a transition between non-adjacent states is about 0.013. From the value for $\langle P_{\text{adj},s} \rangle_s$ given above, one would expect a higher overall probability (about 0.05) for transitions among non-adjacent states. However, this apparent discrepancy is explained by the fact that in 88% of all transitions only the states C, O_1, O_2 and O_3 are involved. For these states, transitions to non-adjacent states occur very seldom.

The probabilities for observing transitions to non-adjacent states (especially for transitions from the closed state to state O_2 or multiples of state O_1) have to be compared to the probability that an intermediate dwelling in an adjacent state is missed. This probability was obtained in the fashion established in Appendix 2 of Ref. [32]: The mean frequency of consecutive transitions was calculated separately for transitions to higher and lower conductance levels. Based on these frequencies and the assumption that the setup cannot capture consecutive events that are spaced closer than the rise time of 11 μs , we obtained a probability of 0.009 (relative to all detected transitions) that two consecutive transitions appear as a single one. This is the same

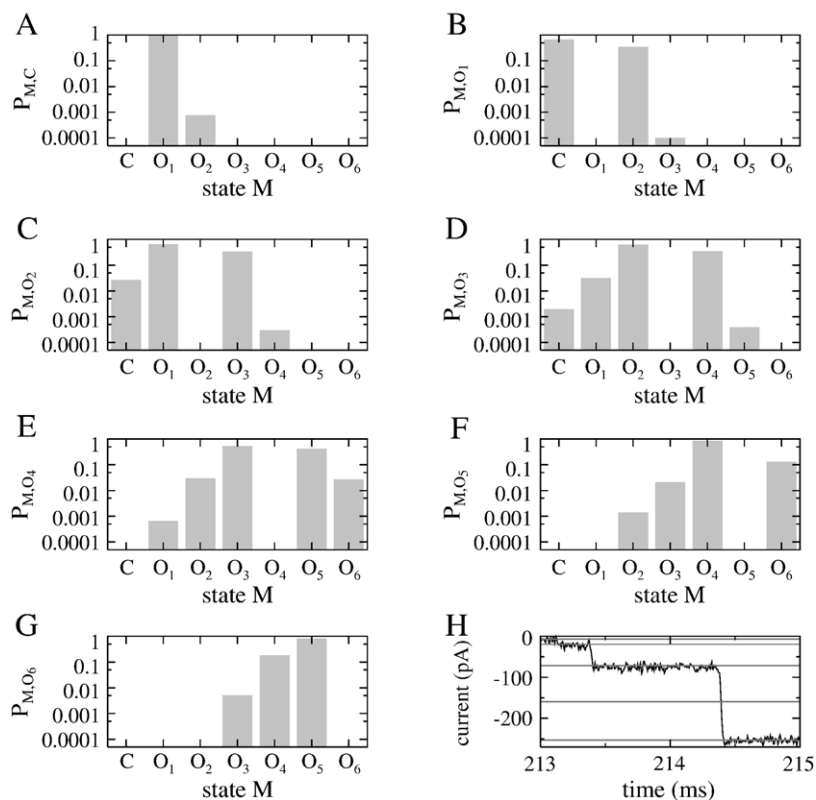


Fig. 4. (A)–(G) Probability $P_{M,N}$ that state N is entered from state M. The probability is relative to all transitions into state N. The data are the same as the ones analyzed in Fig. 3. (H) Example of a transition between non-adjacent states. The displayed time series is a part of the one of Fig. 2A.

order of magnitude as the probability with which transitions between non-adjacent levels were found experimentally.

Qualitatively similar statistical properties of the transitions between the different single-channel states and of the first state occurring after a voltage step were also found for other voltages, voltage jumps from non-zero potential, different alamethicin concentrations or lipid mixtures containing cholesterol. Furthermore, the statistical properties of the inter-state transitions described here were also found in steady-state and in experiments where always only one channel was open. However, detailed measurements on possible dependencies of the experimental findings on voltage, alamethicin concentration or peptide composition are beyond the scope of this paper.

4. Discussion

4.1. Planar patch clamp chips as a substrate for high resolution bilayer recordings

We have shown that our planar patch clamp system, using microstructured glass substrates (patch clamp chips), is capable of analyzing voltage-dependent alamethicin channel gating following step changes in membrane voltage, and of resolving channel openings down to dwell times well below 100 μ s. As used here, i.e., without any modifications, the planar patch clamp system shows unusually high bandwidth and low noise compared to classical bilayer setups. Also, the ability to form solvent-free bilayers from GUVs in an automated fashion is attractive. In addition, with the

glass chips used here, patch clamp experiments with cells as well as with artificial bilayers can be performed with the same setup without the need for any modification. On the other hand, the performance of the present system (5 pA rms noise at 30 kHz) is still much inferior to the best low-noise patch-clamp recordings with pipettes [33,34], which show 6 μ s temporal resolution and 1.5 pA rms noise at 61 kHz filter cutoff, and 12.7 pA rms noise and 3 μ s temporal resolution at 250 kHz filter cutoff, respectively. However, those results were obtained after substantial modifications of headstage and amplifier hardware and the use of non-standard quartz glass pipettes. In contrast, our present recording situation is a pragmatic compromise between several desiderata (low noise, high bandwidth, high current amplitude range, ease of use). A large component of noise in our present setting comes from the input headstage of the amplifier operating with the 500 M Ω feedback resistor. Even when the capacitive load was minimized (open headstage) this was 4.3 pA rms at 30 kHz, i.e., nearly 90% of our total noise figure of approximately 5 pA rms. The required amplitude range in recording alamethicin currents did not allow us to use the feedback resistor of 50 G Ω , which shows an open headstage noise at 30 kHz of approximately 1 pA. In the latter setting, we observed a linear increase in rms noise with the increased capacitive load conferred by the wire connecting the headstage to the chip holder inside the Port-a-Patch housing (+1.8 pF) and the chip holder with the Ag/AgCl-electrode (+1.3 pF) from 1 (0.35) to 1.92 (0.72) and to 2.7 (0.94) pA rms at 30 (10) kHz, respectively. An added noise contribution of the chip capacitance (0.5 pF) was not detectable. Reducing the total capacitance should

be possible by optimizing the design of the connection between headstage and chip but seems warranted only when the 50 G Ω feedback resistor (or alternatively, capacitive feedback [9]) can be used. Extrapolating the linear relationship between capacitance and noise reported above would result in an rms noise current at zero capacitance of 0.27 pA at 30 kHz or 0.11 pA at 10 kHz. These values might be roughly halved when a capacitive feedback amplifier is used [9]. However, they would still be much higher than the $R_c C_F$ noise expected from a bilayer capacitance of 4 fF and 1 M Ω access resistance (about 14 fA, according to Eq. 10 in [9]). This term, which is the most important noise source in classical bilayer recording [35] is therefore essentially eliminated with the setup used here.

Our findings are in agreement with a recent study using micron-sized apertures formed in Teflon membranes [6]. With their smallest (approximately 2 μ m diameter) apertures, these authors found an rms noise of about 1 pA at 10 kHz or 0.44 pA at 4.35 kHz using a capacitive feedback amplifier. The former value can be directly compared to our noise figure of 1 pA rms at 10 kHz using the 50 G Ω feedback resistor. Similar to our findings, these authors obtained a linear relationship between total capacitive load on the headstage and rms noise and concluded that the capacitance of the bilayer does no longer contribute. The total capacitive load in that study was reported to be considerably higher than in our case (19 pF as opposed to 3.15 pF). This disadvantage might be partly offset by the lower intrinsic noise of the capacitive feedback amplifier used.

To our knowledge, the lowest noise figures in planar bilayer recording to date were reported by Akeson et al. [36]. Using 25 μ m diameter (or even smaller) apertures at one end of a Teflon tube connecting two small (70 μ l) baths, they report 0.6 pA using resistive and 0.2 pA rms using capacitive feedback at 5 kHz bandwidth. These values are almost identical to those we obtain after post hoc 5 kHz digital 4-pole Bessel filtering of data obtained at 30 kHz cut-off using the Bessel filter routine from LabView (National Instruments, Vs. 3.1): 0.62 pA and 0.36 pA rms for the 500 M Ω and the 50 G Ω feedback resistor, respectively.

Finally, the silicon chip system used in Ref. [7] should in principle exhibit performance characteristics that are similar to the ones of our system. However, the use of the insulator glass as the chip material has the advantage of a lower intrinsic capacitance in comparison to the semiconductor silicon [2].

4.2. Alamethicin channel formation

There exist several models for the formation of alamethicin channels into lipid membranes [12,37,38,39,40]. These can be divided into two classes. In one class of models it is assumed that alamethicin monomers do not form any aggregates before voltage application [37,40]. The other class of models assumes non-conducting aggregates at zero applied potential [12,38,39]. In the first class of models, the lowest conducting state is formed when a minimum number of monomers assemble to form a conducting pore. Transitions between different conductance states occur by uptake or release of single monomers. In the second class of models, the monomers assemble before the

voltage is applied and inter-state transitions occur due to conformational changes of the aggregates.

The well-known inverse dependence of voltage threshold on alamethicin peptide concentration (see Ref. [20] for a review) in itself is a clear indication that channel opening requires the formation of multimeric aggregates of independent units. In addition, the geometric series of single channel conductance levels strongly suggests that conductance grows with increasing number of monomers per aggregate. Thus, if aggregates do form in the absence of membrane polarization, then the number of monomers per aggregate would be expected to show a distribution similar to that of the conductance states observed in the polarized state. Therefore, upon application of a voltage step, the amplitude of the first observed opening could in principle correspond to any of these conductance states and would not be restricted to the smallest one (O_1). First openings, however, were almost exclusively ($P > 0.98$) to O_1 , while apparent first openings to O_2 were observed with a probability on the order of 0.01, (other states were not observed as first openings). In contrast, the overall probability ratio for states O_1 and O_2 in these recordings was approximately 2 (see Fig. 2). This wide discrepancy in the overall distribution of states and that of the first opening seems difficult to reconcile with models where voltage-dependent opening of alamethicin-channels occurs by conformational transitions of pre-existing aggregates. It is in principle possible that preformed large aggregates can assume multiple conductance states with multiple voltage-dependent transitions between them. However, such a model cannot explain the characteristic reduction of voltage threshold with higher peptide concentrations in channel forming, nor does it offer an easy explanation for the geometric series of conductances.

The low but finite probability found for transitions between non-adjacent conductance states could be taken as an argument against models without preaggregates. However, the observed probabilities for such transitions are rather low, so that they might also be explained by the uptake/release of more than one monomer into/from an existing pore due to diffusion. Furthermore, most of these events are likely due to transitions to adjacent levels which appear too close in time to be properly resolved. Therefore, we conclude that our experimental observations are in good agreement with models that do not rely on the existence of non-conducting preaggregate states.

Acknowledgments

We gratefully acknowledge stimulating discussions with M. Lindemann and Dr. M. Winterhalter, Bremen. We thank Dr. U. Fröbe, Freiburg, for helpful advice on filters and W. Rohm for expert technical assistance. M. S. and J.C. B. acknowledge financial support from the Deutsche Forschungsgemeinschaft within the framework of the SFB 505 and from the University of Freiburg.

References

- [1] B. Sakman, E. Neher (Eds.), *Single-Channel Recordings*, Plenum Press, New York, 1983.
- [2] N. Fertig, R.H. Blick, J.C. Behrends, Whole cell patch clamp recording performed on a planar glass chip, *Biophys. J.* 82 (2002) 3056–3062.

- [3] K.G. Klemic, J.F. Klemic, F.J. Sigworth, An air-molding technique for fabricating pdms planar patch-clamp electrodes, *Pflugers Arch.* 449 (2005) 564–752.
- [4] N. Fertig, M. Klau, M. George, R.H. Blick, J.C. Behrends, Activity of single ion channel proteins detected with a planar microstructure, *Appl. Phys. Lett.* 81 (2002) 4865–4867.
- [5] R. Pantoja, D. Sigg, R. Blunck, F. Bezanilla, J.R. Heath, Bilayer reconstitution of voltage-dependent ion channels using a microfabricated silicon chip, *Biophys. J.* 81 (2001) 2389–2394.
- [6] M. Mayer, J.K. Kriebel, M.T. Tosteson, G.M. Whitesides, Microfabricated teflon membranes for low-noise recordings of ion channels in planar lipid bilayers, *Biophys. J.* 85 (2003) 2684–2695.
- [7] C. Schmidt, M. Mayer, H. Vogel, A chip-based biosensor for the functional analysis of single ion channels, *Angew. Chem., Int. Ed.* 39 (2000) 3137–3140.
- [8] F.J. Sigworth, K.G. Klemic, Microchip technology in ion-channel research, *IEEE Trans. Nanobioscience* 4 (2005) 121–127.
- [9] R.A. Levis, J.L. Rae, Low-noise patch-clamp techniques, *Methods Enzymol.* 293 (1998) 218–266.
- [10] S.B. Hladky, L.G.M. Gordon, D.A. Haydon, Molecular mechanisms of ion transport in lipid membranes, *Annu. Rev. Phys. Chem.* 25 (1974) 11–38.
- [11] P. Mueller, Membrane excitation through voltage-induced aggregation of channel precursors, *Ann. N. Y. Acad. Sci.* 264 (1975) 247–264.
- [12] G. Boheim, W. Hanke, G. Jung, Alamethicin pore formation: voltage-dependent flip-flop of α -helix dipoles, *Biophys. Struct. Mech.* 9 (1983) 181–191.
- [13] R.J. Taylor, R. de Levie, “Reversed” alamethicin conductance in lipid bilayers, *Biophys. J.* 59 (1991) 873–879.
- [14] F.J. Sigworth, D.W. Urry, K.U. Prasad, Open channel noise. iii. high-resolution recordings show rapid current fluctuations in gramicidin a and four chemical analogues, *Biophys. J.* 52 (1987) 1055–1064.
- [15] N. Fertig, C. Meyer, R.H. Blick, C. Trautmann, J.C. Behrends, Microstructured glass chip for ion-channel electrophysiology, *Phys. Rev., E* 64 (2001) 040901.
- [16] M.I. Angelova, Liposome electroformation, in: P.L. Luisi, P. Walde (Eds.), *Giant Vesicles*, John Wiley and Sons Ltd, Chichester, 2000, pp. 27–36.
- [17] A. Brueggemann, M. George, M. Klau, M. Beckler, J. Steindl, J. Behrends, N. Fertig, Ion channel drug discovery and research: the automated nano-patch-clamp© technology, *Curr. Drug Discov. Technol.* 1 (2004) 91–96.
- [18] R. Latorre, O. Alvarez, Voltage-dependent channels in planar lipid bilayer membranes, *Physiol. Rev.* 61 (1981) 77–150.
- [19] G.A. Woolley, B.A. Wallace, Model ion channels: gramicidin and alamethicin, *Membr. Biol.* 192 (1992) 109–136.
- [20] H. Duclouhier, H. Wróblewski, Voltage-dependent pore formation and antimicrobial activity by alamethicin and analogues, *J. Membr. Biol.* 184 (2001) 1–12.
- [21] P. Mueller, D.O. Rudin, Action potentials induced in biomolecular lipid membranes, *Nature* 217 (1968) 713–719.
- [22] A. Mauro, R.P. Nanavati, E. Heyer, Time-variant conductance of bilayer membranes treated with monazomycin and alamethicin, *Proc. Natl. Acad. Sci. U. S. A.* 69 (1972) 3742–3744.
- [23] P. Mueller, Molecular aspects of electrical excitation in lipid bilayers and cell membranes, *Horiz. Biochem. Biophys.* 2 (1976) 230–284.
- [24] G. Boheim, H.-A. Kolb, Analysis of the multi-pore system of alamethicin in a lipid membrane, *J. Membr. Biol.* 38 (1978) 99–150.
- [25] J.E. Hall, M.D. Cahalan, Calcium-induced inactivation of alamethicin in asymmetric lipid bilayers, *J. Gen. Physiol.* 79 (1982) 387–409.
- [26] L.J. Bruner, J.E. Hall, Pressure effects on alamethicin conductance in bilayer membranes, *Biophys. J.* 44 (1983) 39–47.
- [27] B. Schuster, D. Pum, O. Braha, H. Bayley, U.B. Sleytr, Self-assembled α -hemolysin pores in an s-layer-supported lipid bilayer, *Biochim. Biophys. Acta* 1370 (1998) 280–288.
- [28] D. Colquhoun, F.J. Sigworth, Fitting and statistical analysis of single-channel records, in: B. Sakmann, E. Neher (Eds.), *Single-Channel Recording*, Plenum Press, New York, 1995, pp. 483–587.
- [29] G. Boheim, Statistical analysis of alamethicin channels in black lipid membranes, *J. Membr. Biol.* 19 (1974) 277–303.
- [30] W. Hanke, G. Boheim, The lowest conductance state of the alamethicin pore, *Biochim. Biophys. Acta* 596 (1980) 456–462.
- [31] M. Eisenberg, M.E. Kleinberg, J.H. Shaper, Channels across black lipid membranes, *Ann. N. Y. Acad. Sci.* 303 (1977) 281–291.
- [32] N. Ankri, P. Legendre, D. Faber, H. Korn, Automatic detection of spontaneous synaptic responses in central neurons, *J. Neurosci. Methods* 52 (1994) 87–100.
- [33] F. Parzefall, R. Wilhelm, M. Heckmann, J. Dudel, Single channel currents at six microsecond resolution elicited by acetylcholine in mouse myoballs, *J. Physiol.* 512 (1998) 181–188.
- [34] G. Shapovalov, H.A. Lester, Gating transitions in bacterial ion channels measured at 3 μ s resolution, *J. Gen. Physiol.* 124 (2004) 151–161.
- [35] W.F. Wonderlin, A. Finkel, R.J. French, Optimizing planar lipid bilayer single-channel recordings for high resolution with rapid voltage steps, *Biophys. J.* 58 (1990) 289–297.
- [36] M. Akeson, D. Branton, J.J. Kasianowicz, E. Brandin, D.W. Deamer, Microsecond time-scale discrimination among polycytidylic acid, polyadenylic acid, and polyuridylic acid as homopolymers or as segments within single rna molecules, *Biophys. J.* 77 (1999) 3227–3233.
- [37] G. Baumann, P. Mueller, A molecular model of membrane excitability, *J. Supramol. Struct.* 2 (1974) 538–557.
- [38] R.O. Fox, F.M. Richards, A voltage-gated ion channel model inferred from the crystal structure of alamethicin at 1.5-Å resolution, *Nature* 300 (1982) 325–330.
- [39] J.E. Hall, I. Vodyanoy, T.M. Balasubramanian, G.R. Marshall, Alamethicin. a rich model for channel behavior, *Biophys. J.* 45 (1984) 233–247.
- [40] V. Rizzo, S. Stankowski, G. Schwarz, Alamethicin incorporation in lipid bilayers: a thermodynamic study, *Biochemistry* 26 (1987) 2751–2759.